

Solder Creep-Fatigue Interactions With Flexible Leaded Parts

R. G. Ross, Jr.

L. C. Wen

G. R. Mon

E. Jetter

Jet Propulsion Laboratory,
Pasadena, CA 91109

With flexible leaded parts, the solder-joint failure process involves a complex interplay of creep and fatigue mechanisms. To better understand the role of creep in typical multi-hour cyclic loading conditions, a specialized non-linear finite-element creep simulation computer program has been formulated. The numerical algorithm includes the complete part-lead-solder-PWB system, accounting for strain-rate dependence of creep on applied stress and temperature, and the role of the part-lead dimensions and flexibility that determine the total creep deflection (solder strain range) during stress relaxation. The computer program has been used to explore the effects of various solder creep-fatigue parameters such as lead height and stiffness, thermal-cycle test profile, and part/board differential thermal expansion properties. One of the most interesting findings is the strong presence of unidirectional creep-ratcheting that occurs during thermal cycling due to temperature dominated strain-rate effects. To corroborate the solder fatigue model predictions, a number of carefully controlled thermal-cycle tests have been conducted using special bi-metallic test boards.

Introduction

For most spacecraft electronics it is not a single high stress event that breaks a component solder joint; rather it is repeated or prolonged load applications that result in fatigue or creep failure of the solder. Figure 1 presents representative fatigue-life data for 63-37 Sn-Pb solder and illustrates the typical dependency between cycles-to-failure and the total peak-to-peak strain range per cycle. In most electronic packaging applications, the principal strain in solder joints is caused by differential expansion between the part and its mounting environment due to changes in temperature (thermal cycles) and/or due to temperature gradients between the part and the board.

The function of strain relief elements—such as the flexible metals leads of the electronic components—is to lower the differential-expansion induced loads (stresses) on the solder joints to levels below the solder yield strength, thus minimizing the generation of plastic strain. Unfortunately, under typical multi-hour loading conditions the solder joints can still be expected to undergo modest levels of strain due to creep of the solder in response to the applied elastic forces from the strain relief elements. This creep-induced strain has the same damaging effect as more immediately induced plastic strain, and must be summed with the plastic strain to achieve the total plastic strain range that is correlated with fatigue life in Fig. 1.

Because of creep effects, the total strain range during any given loading cycle can be a strong function of solder temperature, the loading time per cycle, the applied solder stress,

and the spring constant of the strain relief elements; in addition, solder metallurgical state including grain size and aging condition also influence the solder creep rate. Figure 2 illustrates the strong dependence of solder strain rate (creep rate) on the temperature of the solder and the stress applied to the solder by the electronic part-board system.

Although extensive research in recent years has led to an increasingly mature understanding of the creep-fatigue properties of solder as an engineering material, much less headway has been made in quantifying solder creep-fatigue behavior at the electronic package systems level. The objective of the on-

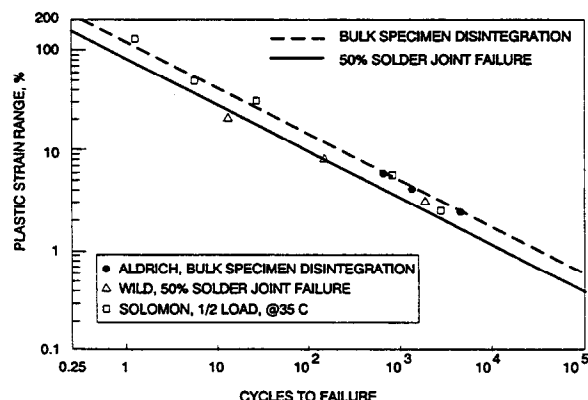


Fig. 1 Coffin-Manson curves fitted to typical eutectic Sn-Pb solder fatigue data from Aldrich (1970), Wild (1975), and Solomon (1990)

Contributed by the Electrical and Electronic Packaging Division and presented at the Winter Annual Meeting, Atlanta, Ga. December 1-6, 1991 of THE AMERICAN SOCIETY OF MECHANICAL ENGINEERS. Manuscript received by the EEPD August 1991. Paper No. 91-WA/EEP-27.

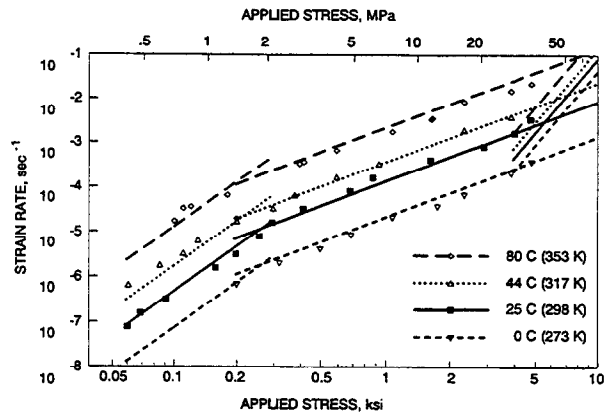


Fig. 2 Eutectic Sn-Pb solder creep strain rate versus applied stress and temperature (from Cline and Alden, 1967)

going study described here is to explore and understand the complex systems-level creep-fatigue interactions involved in electronic part solder joints, and in particular to understand the key solder-joint structural configuration and environmental stress dependencies. Important issues include the effects of component lead flexibility, solder joint geometry, operating temperature, thermal cycling depth, and cyclic frequency of loading. Understanding these issues is important to both achieving robust electronic packaging designs that meet the end-use requirements, and to defining and interpreting appropriate testing procedures for hardware qualification.

The study reported here involves two major elements: 1) the development and use of a specialized non-linear finite-element creep simulation computer program for solder systems analysis, and 2) the development and use of special bi-metallic test boards to conduct accelerated thermal-cycle tests to corroborate the analytical results.

Creep Simulation Modeling

In studying the durability of solder joints, many important parameters such as dependence on component leads and interconnection geometry, cyclic frequency dependence, and temperature dependence, have been shown to be structural-system issues as much as they are materials issues (Ross et al., 1991).

With this premise, the approach of the present study has been to utilize a special purpose nonlinear finite-element elastic-plastic-creep simulation program to study the behavior of solder joints in the context of the complete part-lead-solder-PWB system. Given a time history of environmental loading (e.g., part temperature versus time) the JPL-developed program computes the resulting strain in each element of the solder joint as a function of time. Varying the system geometry, cycle rate, thermal-cycle depth, or any of a wide variety of parameters, allows the resulting effects on solder strain history to be observed directly.

In operation, the program divides the time response of the solder joint into thousands of tiny time increments; for each time increment the solder's incremental plastic strain response is computed based on the existing stress in the solder, the solder's temperature, and the state of externally applied loads. The program starts each time increment by computing the instantaneous stress in each solder element using a special-purpose finite element elastic structural model of the computer part-lead-solder-PWB system. The forcing function for the stresses is the instantaneous geometry of the package system including previously accrued plastic deformation of the solder elements and lead deflections applied externally by thermal-cycle differential expansions or mechanical (isothermal) cycling. Following computation of the stress, the program uses constitutive equations for solder (a numerical expression of

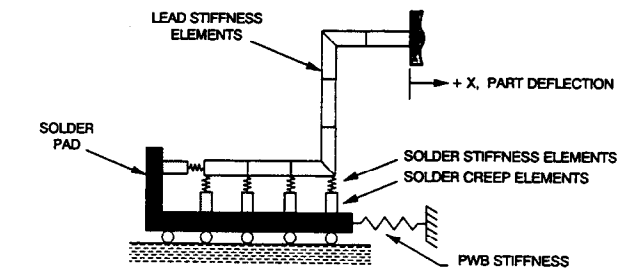


Fig. 3 Schematic of finite element elastic-plastic-creep model of solder joint with gull-wing lead

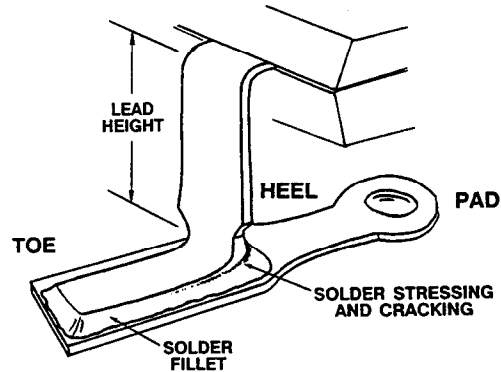


Fig. 4 Solder-joint nomenclature and dimension definitions for flat-pak parts mounted with gull-wing leads

Fig. 2) together with the current solder temperature to compute the plastic strain rate in each solder element, and thus the solder incremental strain during the time interval. A key feature of the program is the dynamic adjustment of the time increment to insure near-constant strain-rate during any given time increment. This is necessary to prevent strain integration errors and model instabilities caused by excessive stress relaxation during any given time interval. In general, the simulations presented in this paper involve incremental time steps ranging from 0.001 second to 1 minute, thus leading to as many as one million strain-increment solutions per simulation run. The shortest time increments are generally required during periods of elevated temperature where stress relaxation occurs rapidly.

Because of the heavy computational load presented by the algorithm, the finite element description of the solder system has been carefully simplified to preserve the important structural and geometric features of the solder system, while sacrificing non-critical spacial detail within the solder joint itself. Figure 3 schematically illustrates the resulting two-dimensional finite element model of the gull-wing lead used in this study. Solder-joint nomenclature for the gull-wing lead is presented in Fig. 4.

Typical Strain Simulation Results

Figure 5 displays the computed strain response during a representative field-application thermal cycle with 15°C temperature range (25°C to 40°C) and 3-hr cyclic period. The input horizontal displacement (δ as defined in Eq. (1)) corresponds to the thermal mismatch between a ceramic flat-pak ($L = 1.23$ cm, $\alpha_p = 6$ ppm/°C) and an Fr₄ PWB bonded to an aluminum substrate ($\alpha_b = 20$ ppm/°C).

$$\delta = L(\alpha_p - \alpha_b)(T - T_0) \quad (1)$$

where

- L = Characteristic length of the lead/solder system
- α_b = Coef. of Thermal Expansion (CTE) for the PWB
- α_p = Effective CTE for the part and leads

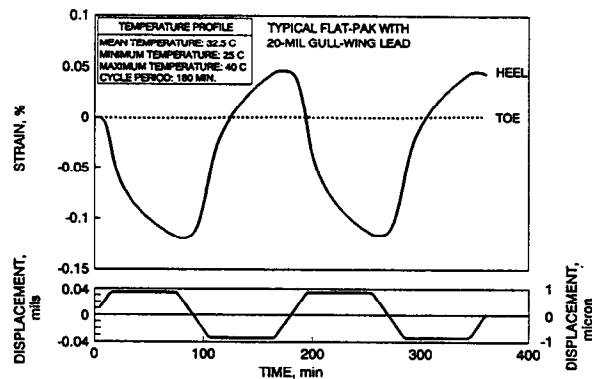


Fig. 5 Example flat-pak lead displacement and solder strain response to 15°C thermal cycle with 3-hour period

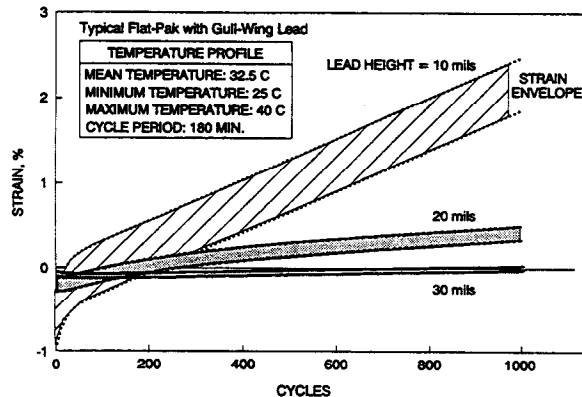


Fig. 6 Thermal cycle strain response showing dependence of creep ratcheting on lead height

T_0 = Reference (no strain) temperature
 T = Instantaneous cyclic temperature

The reference temperature T_0 is taken as 32.5°C and the displacement variation, shown at the bottom of Fig. 5, corresponds to a $\pm 7.5^\circ\text{C}$ temperature swing over the three-hour cycle. The first two cycles of computed strain variation at the solder joint heel and toe are shown in the top of Fig. 5 for a typical 20-mil lead height and 7-mil lead thickness. The maximum strain range (about 0.17 percent) occurs as a normal-to-the-board tension-compression at the heel, while the toe undergoes much less strain.

An example of the use of the program to examine electronic packaging systems effects, Fig. 6 displays the straining at the heel for the same flat-pak part used in Fig. 5, but bent with three different lead heights. Lead stiffness rapidly decreases with increasing lead height for a given lead thickness, thus reducing the solder stress and resulting strain rate. As can be seen, lead stiffness plays a key role in solder joint integrity. For the 10-, 20-, and 30-mil lead heights, the computed cyclic strain ranges are 0.62 percent, 0.16 percent, and 0.051 percent, respectively.

Creep Ratcheting

Perhaps the most important finding from the solder strain simulation results illustrated in Fig. 6 is the existence of progressive strain drift or "creep ratcheting" that accompanies the alternating fatigue component in long-term thermal cycling. In this example, this progressive strain drift is 2.5, 0.5, and 0.04 percent, respectively, after 1000 thermal cycles. An important part of the ongoing research at JPL has been validating this observed phenomenon and understanding its implications on electronic package design and testing. In this

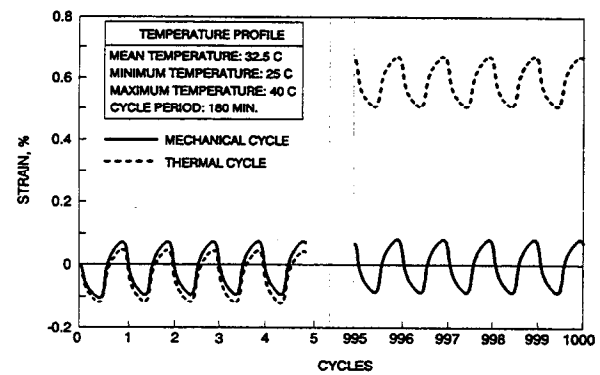


Fig. 7 Creep ratchet visible in thermal-cycle strain response as compared with isothermal mechanical cycling

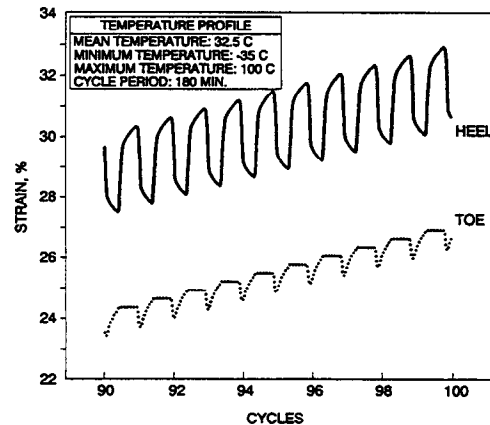


Fig. 8 Creep ratcheting apparent in heel and toe strain response to 135°C thermal cycling

paper we refer to the phenomenon as "creep ratcheting" in recognition of its ratchet-like directional dependence, which stems from the strong temperature dependence of creep during different phases of the loading cycle. Creep ratcheting has proven to be real to our satisfaction, and also agrees with the recent observations of other investigators such as Pan (1991).

To further illustrate the observed creep ratcheting phenomenon, a pair of simulations is presented in Fig. 7, based on the same 20-mil flat-pak used in Fig. 5, but with the displacements provided in one case by the 25°C to 40°C thermal cycle, and in the other case by an isothermal mechanical cycle with the same lead displacement and 32.5°C mean temperature. The left side of the figure compares the strain variations in the first five cycles. It can be seen that the shapes and amplitudes of the two cases are very similar. However, after 1000 cycles, the mechanically cycled straining remains essentially unchanged and is symmetrical about the neutral position. The thermally cycled straining, on the other hand, has ratcheted—in essence, drifted—an additional 0.6 percent over and above the mechanical cycling component.

The mechanics of creep-ratcheting can be better understood by studying the exaggerated movements occurring in deep temperature cycles (-35°C to 100°C); these are typical of NASA qualification test levels for electronic circuit boards (NASA, 1986).

Figure 8 displays the tension-compression strain variations occurring between the 90th and 100th deep thermal cycle (range = 135°C , mean temperature = 32.5°C) as computed at the heel and at the toe for the same lead-solder system used in Fig. 6. The rate of creep ratcheting is considerably larger for the 135°C cycle depth than for the 15°C cycle depth; this can be seen by comparing the data of Figs. 6 and 8. Note that the

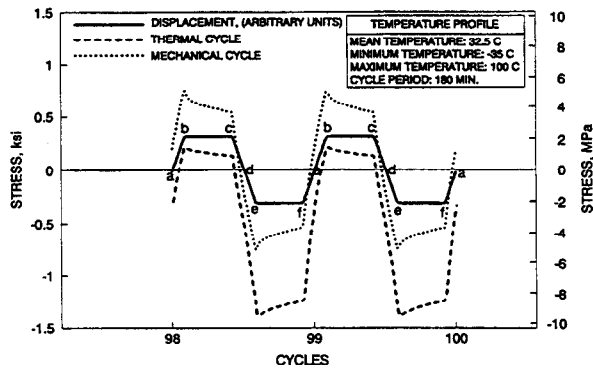


Fig. 9 Comparison of steady state shear stress vs. time for isothermal mechanical cycling and thermal cycling having the identical (shown) displacement

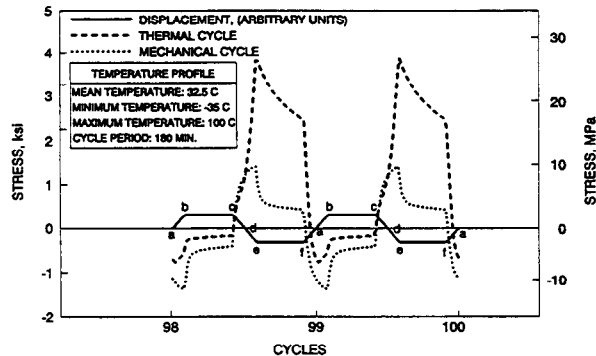


Fig. 10 Comparison of steady state heel stress versus time for isothermal mechanical cycling and thermal cycling having the identical (shown) displacement

tension-compression strains at the heel and toe are out of phase; when the heel fillet is in tension, the toe fillet is in compression, and vice versa. Thus the foot of the lead, which is directly connected to the solder, rocks back and forth (heel-to-toe) while at the same time, because of the creep ratcheting of the solder, it suffers a bias "drift" in a direction normal to the board—away from the board if $\alpha_b > \alpha_p$, toward the board if $\alpha_b < \alpha_p$.

To explore the fundamentals underlying the creep-ratcheting phenomenon, it is useful to examine closely the 135°C thermal-cycle simulation results. Figure 9 shows the computed shear stress variations for this thermal cycle (for $\alpha_b > \alpha_p$) overlaid on the corresponding data for isothermal mechanical cycling, i.e., with identical part displacement profiles. It is helpful to first examine the mechanics of the mechanical cycling, and then to contrast them with the observed differences for thermal-cycling.

Strain Development During Isothermal Mechanical Cycling. During the expansion phase of the isothermal mechanical cycle, there is a positive displacement of the part lead in the $+x$ direction (see Fig. 3), and a resulting horizontal force applied to the solder fillet in the $+x$ direction. This force generates both horizontal shear stresses and vertical tension-compression stresses within the solder. The corresponding shear stress in the solder increases to a maximum as the displacement proceeds from point "a" to point "b" (Fig. 9). During the dwell time ("b" to "c"), the stress relaxes due to creep until the displacement direction reverses ("c" to "d") and ultimately achieves a maximum displacement in the $-x$ direction (point "e") just before the stress again undergoes creep relaxation during the dwell period. In essence, once a steady state condition is achieved, the shear stress variation during isothermal mechanical cycling is symmetrical relative to the neutral position and it closely tracks the displacement profile.

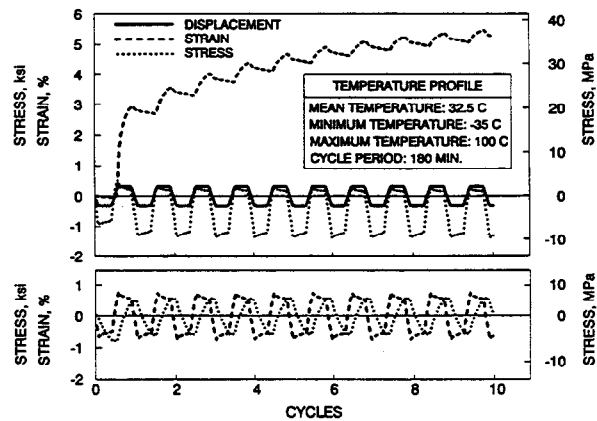


Fig. 11 Transient shear stress and strain response to isothermal mechanical cycling (bottom) and thermal cycling (top) with identical displacement

The corresponding tension-compression heel stress variation in isothermal mechanical cycling is also symmetrical about the zero strain axis, as shown in Fig. 10. The heel is under compression, while the toe is under tension when the part displacement is positive. These stresses relax during the dwell time and reverse their sense when the part displacement changes direction.

Strain Development During Thermal Cycling. If the part displacements arise from differential thermal expansion-contraction during temperature cycling, the dynamics are quite different from those for isothermal mechanical cycling; this is because solder creeps much more rapidly during the higher-temperature portion of the cycle than during the lower-temperature portion, in accordance with Fig. 2. The difference between isothermal mechanical cycling and temperature cycling manifests in the very first cycle. If the thermal cycle starts with cooling, a net initial displacement in the $-x$ direction, the solder is quite creep-resistant because of the low temperature; the resulting shear strain is therefore very limited and most of the would-be solder displacement is absorbed by lead deflection. As the solder temperature increases during the warm-up phase of the cycle, it more readily deforms in response to the force exerted by the deflected lead, and produces a large shear strain in the $+x$ direction (almost 3 percent in the first cycle as shown in Fig. 11). In the subsequent cooling phase the solder again loses its ductility and yields only slightly in the reverse ($-x$) direction. After a number of cycles the lead achieves a deflection bias in the $+x$ direction that provides a greater force in the yielding direction during the cold half cycle, and a reduced force during the hot half cycle. This equilibrium force offset is that required to provide equal horizontal creep in plus and minus shear directions during each cycle; at this point the shear strain cycling becomes symmetrical, and this symmetry is a function of the lead stiffness and lead-solder characteristics.

In response to this horizontal lead deflection offset that develops to maintain shear strain symmetry, out of phase tension-compression forces are developed normal to the board favoring tension creep in the solder joint for the case $\alpha_b > \alpha_p$, and compression creep in the solder joint for the case $\alpha_b < \alpha_p$. As a result, the tension-compression stress at the heel during the cooldown, "c-d-e", is significantly larger than the same stress during the warmup, "f-a-b", as shown in Figs. 10 and 12. Consequently, a resultant creep-ratcheting strain in the tension-compression direction is generated each cycle. Since normal-to-the-board tension drift has no means of generating a self-arresting force, it continues ratcheting at a constant rate as illustrated in Fig. 6. For the opposite case ($\alpha_b < \alpha_p$), where normal-to-the-board ratcheting occurs in the compression di-

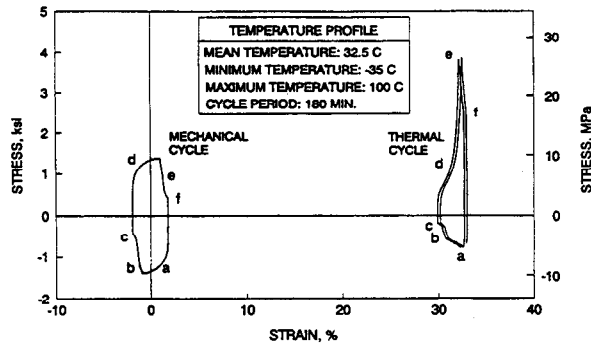


Fig. 12 Heel stress-strain hysteresis loops for thermally and mechanically strained solder joint

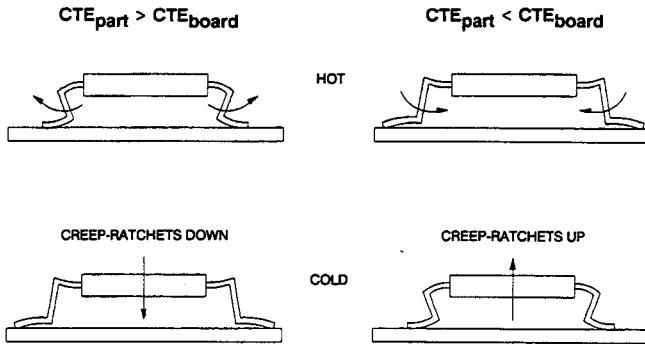


Fig. 13 Visualization of creep-ratchet induced lead deflections and ratchet directions for parts with gull-wing leads

rection, ratcheting will self arrest when the lead bottoms out against the solder pad. These creep-ratchet induced lead deflections and ratchet directions are schematically illustrated in Fig. 13.

Damage Prediction with Combined Creep Ratcheting and Fatigue

Before further examining the implications of the strain simulation results it is useful to develop an analysis structure for comparing the damage caused by creep-ratcheting strain relative to that caused by cyclic fatigue strain.

Although there are many possible approaches to assessing the interactive damage contributions of creep rupture and fatigue, the most straightforward technique is to use Miner's Rule, which additively accumulates the individual fractional damage rates as follows:

$$\phi = \eta N/T + N/N_f = N(\eta/T + 1/N_f) \quad (2)$$

where

- ϕ = fraction of useful service life consumed
- η = creep ratchet strain per cycle
- Γ = strain limit for creep rupture
- N = number of cycles of applied stress
- N_f = number of cycles to fatigue failure

If we use Manson's (1965) fatigue relationship as embodied in Fig. 1 to predict N_f , then

$$N_f^\beta \Delta\epsilon = C \quad (3)$$

where

- N_f = number of cycles to fatigue failure
- $\Delta\epsilon$ = cyclic plastic strain range
- $\beta \approx 0.46$ (from curve slope in Fig. 1)
- $C \approx 0.80$ (for 50 percent solder failure limit in Fig. 1)

To estimate the strain rupture limit (Γ), we again follow the

Table 1. Comparison of computed creep-fatigue damage and predicted life for solder joints with different lead heights and thermal-cycle depths

Lead Height, mils (mm)	Cycle Depth (°C)	Cyclic Strain Range $\Delta\epsilon$, (%)	Creep Ratchet Strain, (%) per 1000 Cycles	50% Failures		
				N	θ , (%)	κ
10 (.25)	15	0.512	2.50	2.9E4	49	1
	135	4.630	683	152	69	195
20 (.51)	15	0.160	0.50	2.1E5	71	1
	135	2.830	330	347	76	618
30 (.76)	15	0.051	0.04	2.6E6	70	1
	135	1.470	9.13	4370	26	607

Cycle period = 180 minutes

N = Service life, cycles

θ = Percent damage due to creep ratcheting

κ = Acceleration factor

lead of Manson, who in the development of his strain-cycle fatigue relationship (Eq. (3)), viewed the tensile test as a cyclic fatigue failure at 1/4 cycle. In similar fashion the strain range at the 1/4-cycle point on the Coffin-Manson plot can be taken as a rough estimate of the creep extension limit, i.e.,

$$\Gamma \approx C/(0.25)^\beta \quad (4)$$

Combining Eqs. (2), (3) and (4) gives

$$\phi = N[\eta(0.25)^\beta/C + (\Delta\epsilon/C)^{1/\beta}] \quad (5)$$

Equation (5) can also be used to describe the acceleration of a particular test condition (1) over that of another condition (2) by noting that the acceleration ratio κ is given by the ratio N_2/N_1 , where N_1 is the number of environmental stress cycles at condition (1) required to yield the same damage as N_2 cycles at environmental stress condition (2), i.e., $\kappa = N_2/N_1$ for $\phi_1 = \phi_2$; thus,

$$\kappa = \frac{[\eta_1(0.25)^\beta/C + (\Delta\epsilon_1/C)^{1/\beta}]}{[\eta_2(0.25)^\beta/C + (\Delta\epsilon_2/C)^{1/\beta}]} \quad (6)$$

Strain Damage Estimates for Combined Creep Ratcheting and Fatigue

Returning to the above examples, Eq. (5) can now be used to obtain an estimate of the relative importance of the observed strain ratcheting and cyclic fatigue.

With the modest 15°C-cycle depth used in Fig. 6, recall that the creep ratcheting drifts were 2.5, 0.5, and 0.04 percent after 1000 cycles for the 10-, 20-, and 30-mil lead heights, respectively, and the corresponding cyclic fatigue strain range per cycle was 0.62, 0.16, and 0.051 percent, respectively. When these data and the parameters from Fig. 1 are entered in Eq. (5), the creep-ratchet and fatigue damage are both found to be quite small, but about equal in level.

Continuing this analysis for the simulation results of the deep 135°C thermal cycles provides the data assembled in Table 1. In the cases presented in Table 1, the dominating failure mechanisms are extension-compression low-cycle fatigue and creep at the heel (or toe) of the solder joints. Note that creep-ratcheting represents over 50 percent of the damage in most of the cases.

For completeness, it is also important to note that under a "worst case" combination of stiff lead, large temperature cycling range, and large mismatch in CTEs, different creep and fatigue mechanisms, those acting in the shear direction, can

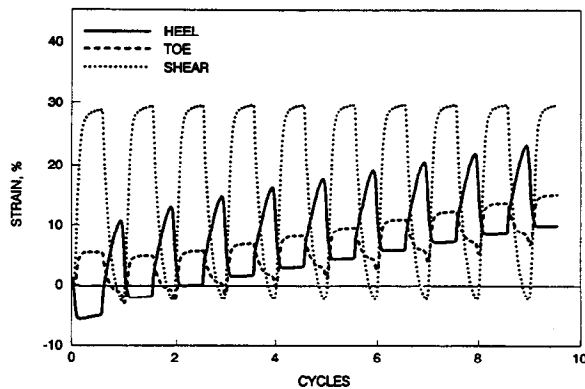


Fig. 14 Dominance of shear strain with flat-pak with stiff 10-mil lead height mounted to type AL/SS test fixture for accelerated thermal-cycle testing

dominate solder joint damage accumulation (Ross et al., 1991). To illustrate this, consider a 10-mil lead height flat-pak assembly on a thermal expansion fixture subjected to a -25°C to $+100^{\circ}\text{C}$ thermal-cycle environment with a 3-hour cycle period. For this case the extension-compression cyclic strain range, shown in Fig. 14, is approximately 15 percent, and the creep ratchet in the normal-to-the-board direction is 15 percent per 100 cycles. However, the dominating contributor to failure is neither of these normal-to-the-board mechanisms. The computed parallel-to-the-board shear strain is as much as 30 percent, and may produce failure in less than 10 cycles, while the damage contribution from extension-compression fatigue and creep rupture is less than 10 percent. Because the dominating failure mechanisms can be significantly different for different thermal-cycle and mechanical-loading environments, care must be exercised in extrapolating test results from one environment to another. This is particularly true for the process of developing and understanding the results of accelerated testing.

Experimental Testing of Creep-Fatigue Interactions

It can be seen from the previous discussion that creep-fatigue interaction is far more complicated than generally anticipated. Just as both temperature range and lead stiffness can significantly influence the relative roles of creep ratcheting and cyclic fatigue, so also can other operational parameters be influential. In particular, the relative direction of creep ratcheting can be extremely important. If creep ratcheting is in the compression direction, the lead will bottom out on the PWB solder pad and the creep will self-arrest. On the other hand, if the creep ratcheting is in the tension direction, the lead may gradually pull out of the solder joint until complete separation occurs.

In order to experimentally investigate the system aspects of combined creep-fatigue interactions, special bi-metallic test fixtures, Fig. 15, were developed. A particularly useful feature of the bi-metallic fixtures is the ability of the relative position of the two metal plates (one aluminum with CTE $\approx 23 \text{ ppm}/^{\circ}\text{C}$, the other a 400-series stainless steel with CTE $\approx 9 \text{ ppm}/^{\circ}\text{C}$) to be reversed; this provides a method to evaluate the level and direction of creep ratcheting. When the stainless steel plate is placed on top of the aluminum, the assembly simulates a low-CTE part mounted to a high-CTE board—this correlates with tensile creep ratcheting away from the solder pads, and the possibility of ultimate tensile failure. If the plates are reversed, the assembly simulates a high-CTE part mounted to a low-CTE board, and the creep ratcheting is in compression, and therefore self arresting against the solder pads.

In order to demonstrate the effect of creep ratcheting, and to validate the service life prediction methodology, a special experiment was conducted with gullwing-leaded flat-paks soldered on the two types of fixtures—the type SS/AL (Stainless

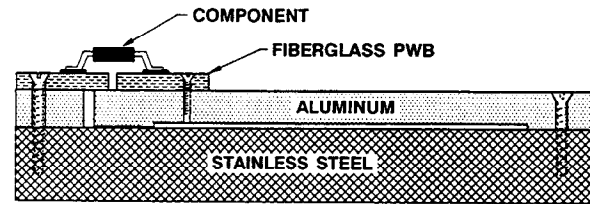


Fig. 15 Bimetallic test fixture for accelerated thermal-cycle testing

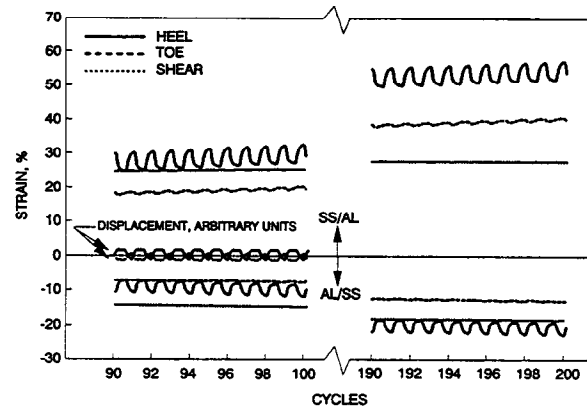


Fig. 16 Strains and displacements versus time for flat-paks with 30-mil (0.76 mm) lead height mounted to indicated fixtures and exposed to thermal cycling from -25°C to $+100^{\circ}\text{C}$

Steel on Aluminum) and the type AL/SS (Aluminum on Stainless Steel). To avoid excessive shear stressing, compliant 5-mil thick by 30-mil high leads were employed in this experiment. The temperature cycling was conducted from -25°C to $+100^{\circ}\text{C}$ using the 3-hr cycle derived for spacecraft electronics qualification (Ross, 1991).

Analytical Predictions. Before starting the test, the finite element strain simulation program was used in conjunction with the failure prediction methodology to analyze and predict the expected outcome. Figure 16 illustrates the shear and normal heel strains computed using the creep-fatigue simulation program for the 90th through the 200th cycle of the -25°C to $+100^{\circ}\text{C}$ thermal-cycle exposure. Note that the lead displacement for the two assemblies move out of phase with each other and their magnitudes are not identical; this is because, even though the contribution of the chip/lead CTE in both cases is the same, the contributions of the bi-metal CTEs are not.

The curves above the zero-strain axis in Fig. 16 show the strain developed in the solder joints on the SS/AL fixture. The dominating strains are seen to be combined cyclic and creep-ratchet tension-compression strain at the solder joint heel, i.e., the toe strains are typically less dominant than the heel strains. One notices that the cyclic heel strain range remains at a constant level of 5.54 percent throughout the testing, i.e., the damage due to low cycle tension-compression fatigue is accruing at a constant rate. Similarly, the creep ratcheting rate for normal strain at the heel is also progressing at a constant rate of 28 percent per 100 cycles. The shear strain, on the other hand, behaves quite differently. The shear cycle strain range is too small (less than 0.2 percent) to account for significant damage contribution, and although the shear creep-ratchet bias is very significant in the early stages of cycling, it reaches a plateau at around $+25$ percent, and grows very little thereafter. After 100 cycles, the damage on the solder joints primarily derives from a combination of tension-compression fatigue and creep ratcheting, with a fixed shear creep-ratchet contribution. Based on Eq. (5), the expected cycles-to-failure due to

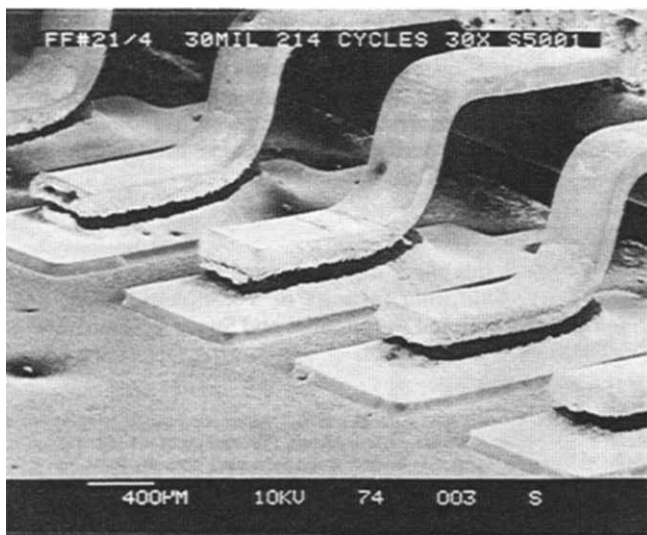


Fig. 17 Failure of solder joints on type SS/AL fixture after 214 thermal cycles from -25°C to $+100^{\circ}\text{C}$

combined creep ratcheting and fatigue is 210 cycles. In this case, the failure is dominated by cyclic fatigue, although creep ratcheting contributes a significant 37 percent to the overall damage.

In contrast, the same solder joints on an AL/SS fixture show a completely different correlation (bottom curves in Fig. 16). For this case, the tension-compression strains creep ratchet in the negative (compression) direction, and the shear strain is also in the opposite (negative) direction from that of the SS/AL fixture. The cyclic shear strain range is only 0.08 percent with a quasi-static creep ratchet displacement of approximately 17 percent. The heel cyclic tension-compression strain range is 3.45 percent, and the corresponding creep-ratcheting compression strain is 10 percent per 100 cycles. Unlike tensile creep ratcheting, compressive creep ratcheting contributes to damage, but is self arresting; consequently, the principal mechanism contributing to failure is cyclic fatigue, and the expected fatigue endurance for a 50 percent failure criterion is approximately 1000 cycles. This is five times that of the inverted SS/AL board.

Thermal Cycle Test Results. After approximately 100 thermal cycles, the test fixtures were removed from the test chamber and examined microscopically. No solder joint failures were evident, but stress lines (fine microcracks) were observed in the fillets as were small cracks at the heels. However, there were no significant visual indications to reflect the analytical prediction that the solder joints on the SS/AL fixture should have a service life only 20 percent of those on the AL/SS fixture.

Again after 164 cycles the fixtures were removed from the test chamber and examined. The solder joints on the SS/AL fixture showed some crack propagation starting from the heel, while the solder joints on the AL/SS fixture remained in essentially the same state they were at after 100 cycles. After around 200 cycles, the solder cracks on the SS/AL fixture reached their rupture limit and began to fail catastrophically. Figure 17 shows the lifted leads as they appeared at 214 cycles, while Fig. 18 shows a cross-section of two of these leads, one lifted and one still surviving. The lead lifting and number of cycles to failure are in good agreement with the tensile creep-ratcheting-fatigue failure predicted above and illustrated in the right side of Fig. 13.

Also as predicted, the solder joints on the AL/SS fixture showed no significant crack growth after 200 cycles, and re-

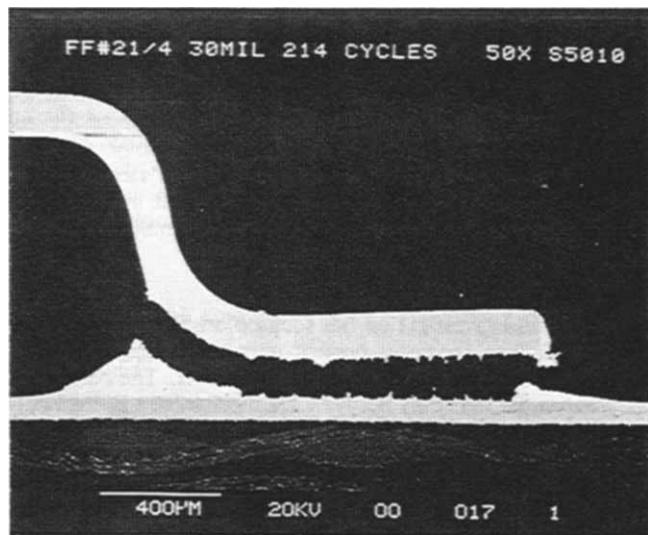


Fig. 18 Cross-section of solder joints on SS/AL fixture displaying tensile failure after 214 cycles

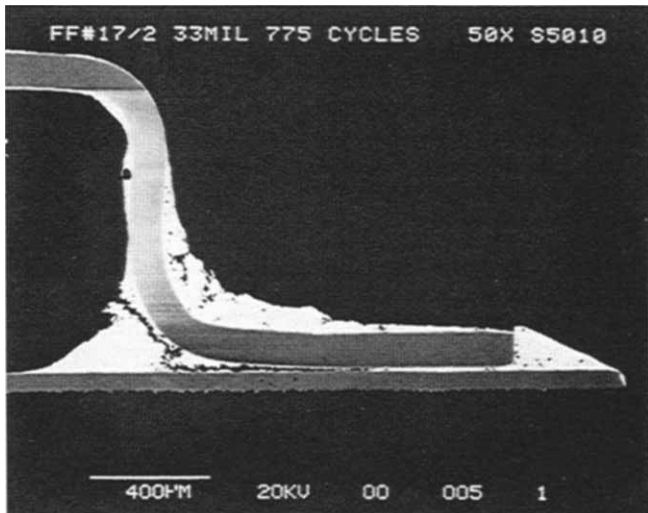


Fig. 19 Cross-section of solder joint on AL/SS fixture displaying compressive creep ratcheting after 775 cycles

mained intact for hundreds of additional cycles. Figure 19 presents a cross-section of a representative solder joint on the AL/SS fixture after 775 cycles. Although crack propagation

has progressed from the heel to the middle of the foot, the toe region is solidly attached and appears compressed toward the board. This agrees with the expectation of negative (compressive) creep-ratcheting as shown in the left side of Fig. 13.

In conclusion, the experimental evidence supports the analytical simulation and life-prediction methodology, and suggests that creep ratcheting is an important system's level damage mechanism that should be carefully addressed in the design and testing of solder joints in electronic assemblies.

Discussion and Concluding Summary

The present investigation has focused on demonstrating the complex failure processes present with creep-fatigue interaction at the electronic package system's level. The results indicate that the interplay between the mechanisms is extremely intricate. For flat-paks having gull-wing leads in thermal cycling environments, creep and fatigue act simultaneously and jointly on the solder joint. The interaction produces a heel-to-toe rocking that causes the lead to lift out of, or plow into, the solder fillet, a phenomenon we have dubbed "creep ratcheting." This phenomenon was not found in simulations of isothermal mechanical cycling.

Lead compliance has been shown to play a profound role in solder joint response to thermal cycling. Solder joints with leads having different compliance are likely to lead to different damage mechanisms in the same test environment. For compliant leads, solder-joint failure in a thermal cycling environment is generally caused by a combination of tension-compression cyclic fatigue and creep ratcheting at the heel. However, for a very stiff lead the dominant damage mechanism can be cyclic shear fatigue.

The relative importance of each damage mechanism can change as the test progresses. Initial shear creep ratcheting, if it does not exceed the rupture limit, is self-arresting after a few cycles. This damage mechanism can thus produce an early appearance of cracks, but does not necessarily result in crack propagation. Instead, as more and more cycles accumulate,

the dominant damage mechanism can become tensile creep ratcheting and fatigue, eventually resulting in failure. An important observation is that conclusions based upon early test inspections, when one failure mechanism is predominant, may lead to erroneous projections of failure at later times; this is because damage accumulation rates change as different mechanisms become predominant.

Acknowledgment

The work in this paper was carried out by the Jet Propulsion Laboratory, California Institute of Technology, under contract with the National Aeronautics and Space Administration.

References

- Aldrich, J. W., and Avery, D. H., 1970, "Alternating Strain Behavior of a Superplastic Metal," *Ultrafine Grain Metals*, Proceedings of the 16th Sagamore Army Material Research Conference, Aug., Syracuse University Press, pp. 397-416.
- Cline, H. E., and Alden, T. H., 1967, "Rate Sensitive Deformation in Tin-Lead Alloy," *Trans. AIME*, Vol. 239, pp. 710-714.
- Mason, S. S., 1960, "Effect of Mean Stress and Strain on Cyclic Life," *Machine Design*, Aug., pp. 129-135.
- Mason, S. S., 1965, "Fatigue: A Complex Subject — Some Simple Approximations," *Engineering Mechanics*, Vol. 5, pp. 193-226.
- NASA, 1986, "Requirements for Soldered Electrical Connections," NHB 5300.4 (3A-1), revalidation date June.
- Pan, T.-Y., 1991, "Thermal Cycling Induced Plastic Deformation in Solder Joints — Part 1: Accumulated Deformation in Surface Mount Joints," *ASME JOURNAL OF ELECTRONIC PACKAGING*, Vol. 113, Mar., pp. 8-15.
- Ross, R. G., Jr., 1991, "A Systems Approach to Solder Joint Fatigue in Spacecraft Electronic Packaging," *ASME JOURNAL OF ELECTRONIC PACKAGING*, Vol. 113, June, pp. 121-128.
- Ross, R. G. Jr., et al., 1991, "Creep-Fatigue Behavior of Microelectronic Solder Joints," *Proceedings of the 1991 MRS Spring Meeting*, Anaheim CA, April 30-May 4, 1991.
- Solomon, H. D., 1990, "Influence of Temperature on the Fatigue of CC/PWB Joints," *Journal of the IES*, Jan./Feb., pp. 17-25.
- Vaynman, S., Fine, M. E., and Jeannotte, D. A., 1991, "Low-cycle Isothermal Fatigue Life of Soldered Materials," *Solder Mechanics*, Ed. by Frear, D. R., et al., The Minerals, Metals & Material Society.
- Wild, R. N., 1975, "Some Fatigue Properties of Solders and Solder Joints," IBM Report No. 7AZ000481, IBM Federal Systems Division, New York.